

Article

N-Skatyltryptamines—Dual 5-HT₆R/D₂R Ligands with Antipsychotic and Procognitive Potential

Agata Hogendorf ¹, Adam S. Hogendorf ¹, Rafał Kurczab ¹, Grzegorz Satała ¹, Bernadeta Szewczyk ², Paulina Cieślak ², Gniewomir Latacz ³, Jadwiga Handzlik ³, Tomasz Lenda ⁴, Katarzyna Kaczorowska ¹, Jakub Staroń ¹, Ryszard Bugno ¹, Beata Duszyńska ¹ and Andrzej J. Bojarski ^{1,*}

- ¹ Department of Medicinal Chemistry, Maj Institute of Pharmacology, Polish Academy of Sciences, 12 Smętna Street, 31-343 Kraków, Poland; agatah@if-pan.krakow.pl (A.H.); ahogen@if-pan.krakow.pl (A.S.H.); kurczab@if-pan.krakow.pl (R.K.); satala@if-pan.krakow.pl (G.S.); k.kaczor@if-pan.krakow.pl (K.K.); staron@if-pan.krakow.pl (J.S.); bugno@if-pan.krakow.pl (R.B.); duszyn@if-pan.krakow.pl (B.D.)
- ² Department of Neurobiology, Maj Institute of Pharmacology, Polish Academy of Sciences, 12 Smętna Street, 31-343 Kraków, Poland; szewczyk@if-pan.krakow.pl (B.S.); cieslik@if-pan.krakow.pl (P.C.)
- ³ Department of Technology and Biotechnology of Drugs, Jagiellonian University Medical College, Medyczna 9, 30-688 Kraków, Poland; glatacz@cm-uj.krakow.pl (G.L.); j.handzlik@uj.edu.pl (J.H.)
- ⁴ Department of Neuropsychopharmacology, Maj Institute of Pharmacology, Polish Academy of Sciences, 12 Smętna Street, 31-343 Kraków, Poland; lenda@if-pan.krakow.pl
- * Correspondence: bojarski@if-pan.krakow.pl



Citation: Hogendorf, A.; Hogendorf, A.S.; Kurczab, R.; Satała, G.; Szewczyk, B.; Cieślak, P.; Latacz, G.; Handzlik, J.; Lenda, T.; Kaczorowska, K.; et al. N-Skatyltryptamines—Dual 5-HT₆R/D₂R Ligands with Antipsychotic and Procognitive Potential. *Molecules* **2021**, *26*, 4605. <https://doi.org/10.3390/molecules26154605>

Academic Editor: Jérôme Leprince

Received: 1 June 2021

Accepted: 26 July 2021

Published: 29 July 2021

Publisher's Note: MDPI stays neutral with regard to jurisdictional claims in published maps and institutional affiliations.



Copyright: © 2021 by the authors. Licensee MDPI, Basel, Switzerland. This article is an open access article distributed under the terms and conditions of the Creative Commons Attribution (CC BY) license (<https://creativecommons.org/licenses/by/4.0/>).

Abstract: A series of *N*-skatyltryptamines was synthesized and their affinities for serotonin and dopamine receptors were determined. Compounds exhibited activity toward 5-HT_{1A}, 5-HT_{2A}, 5-HT₆, and D₂ receptors. Substitution patterns resulting in affinity/activity switches were identified and studied using homology modeling. Chosen hits were screened to determine their metabolism, permeability, hepatotoxicity, and CYP inhibition. Several D₂ receptor antagonists with additional 5-HT₆R antagonist and agonist properties were identified. The former combination resembled known antipsychotic agents, while the latter was particularly interesting due to the fact that it has not been studied before. Selective 5-HT₆R antagonists have been shown previously to produce procognitive and promnesic effects in several rodent models. Administration of 5-HT₆R agonists was more ambiguous—in naive animals, it did not alter memory or produce slight amnesic effects, while in rodent models of memory impairment, they ameliorated the condition just like antagonists. Using the identified hit compounds **15** and **18**, we tried to sort out the difference between ligands exhibiting the D₂R antagonist function combined with 5-HT₆R agonism, and mixed D₂/5-HT₆R antagonists in murine models of psychosis.

Keywords: *N*-skatyltryptamine; tryptamine; D₂/5-HT₆R receptor agonist/antagonist; antipsychotic; procognitive; halogen bond; serotonin dual ligands

1. Introduction

The 5-HT₆ receptor has gained the attention of the pharma industry as a putative target for novel cognitive enhancers in dementia [1–3] as well as an important co-target in the design of psychotropic drugs. The high affinity of several typical and atypical antipsychotics and tricyclic antidepressants for 5-HT₆, taken together with its sole CNS distribution, notably in the hippocampus, nucleus accumbens, prefrontal cortex, and striatum, has prompted intensive research, which partially revealed the physiological function of the receptor, in particular, its association with GABAergic and cholinergic transmission [4,5].

5-HT₆R blockade has been proposed as a treatment of Alzheimer's disease (AD) symptoms, however, the strategy ultimately failed, with no drugs on the market so far despite intensive clinical trial campaigns led by several companies [6–9]. Given the lack of efficacy of selective 5-HT₆R antagonists in AD, several polypharmacological approaches have been proposed instead [10–15].

Although 5-HT₆R blockade on its own as a procognitive treatment in dementia failed, it is still a matter of debate whether the 5-HT₆R component contributes to a beneficial profile of certain psychotropic drugs [16]. Cognitive decline has been an unresolved symptom of schizophrenia, which prohibits the patients from a return to work and social functioning. Co-administration of a 5-HT₆ antagonist AVN-211 in patients with schizophrenia stabilized on antipsychotic treatment has resulted in an improvement in Positive and Negative Syndrome Scale score over the placebo group [17]. Interestingly, while only antagonists of 5-HT₆R display memory-enhancing properties per se, both agonists and antagonists reverse the cognitive deficits in rodent models of schizophrenia [18–20].

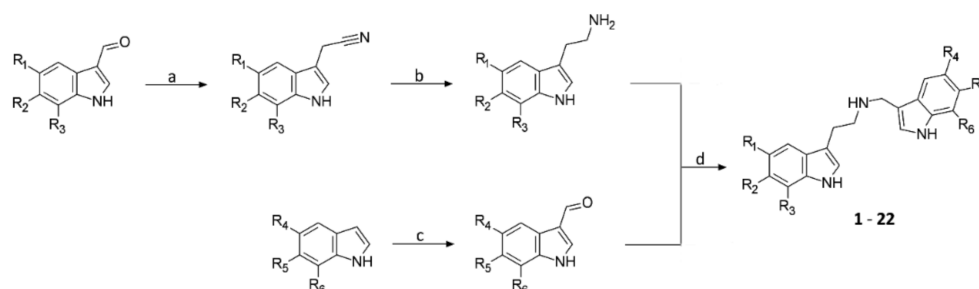
NMDA antagonist administration is a well-established screening model of cognitive deficits resembling the symptoms of schizophrenia [21,22]. Typically, the impairment is induced by phencyclidine (PCP) or dizocilpine (MK-801) [23]. The clinical candidate LU AE58054, a 5-HT₆R antagonist, has been shown to reverse the cognitive impairment induced by subchronic phencyclidine in NORT in rats [24]. Administration of MK-801 resulted in an increase in locomotion, increased pre-pulse inhibition, stereotypy, deficits in spatial memory, and impaired novel object recognition [25]. The effects of the administration of a selective 5-HT₆R antagonist and agonist on MK-801 induced memory impairment in the NOR task have recently been published [20]. It has been shown that, counterintuitively, both ameliorated the MK-801 effects in NORT, which could have been related to the restoration of physiological BDNF levels. Tryptamines represent an important group of compounds exhibiting various biological activities, especially renowned as serotonin receptor ligands. A SAR study of benzyl-5-methoxytryptamines, a chemotype that was investigated due to the structural resemblance to the ultrapotent 5-HT ligands: *N*-benzyl-2,5-dimethoxyphenylethylamines, was published in 2015 by Nichols et al. [26]. Compounds were evaluated as 5-HT_{2A}R ligands, but also screened against several other 5-HT receptors, revealing their promiscuous nature including affinity for 5-HT₆R. Surprisingly, so far, little effort has been put to explore the chemical space of the *N*-arylmethyl-arylethylamines beyond the works that focused on benzyl derivatives of tryptamines and phenylethylamines as 5-HT_{2A}R agonists. In this work, we present a part of our search for non-sulfonyl 5-HT₆ receptor ligands within the aforementioned scaffold. Several mixed D₂/5-HT₆R ligands exhibiting different functional profiles have been discovered, and their ADMET properties explored.

While studying the literature, we did not come across any reports of mixed D₂ antagonist–5-HT₆ agonists in animal models of schizophrenia-related cognitive decline. A compound with such a functional profile–18 was thus compared with a mixed D₂/5-HT₆R antagonist in screening models.

2. Results

2.1. Chemistry

N-skatyltryptamines were synthesized using the procedure shown in Scheme 1. Several monosubstituted aldehydes were commercially available, and the others were synthesized via Vilsmeier–Haack formylation starting from appropriate monosubstituted indoles. The aldehydes were converted into the nitriles in a two-step, one-pot process involving reduction with NaBH₄ and substitution with NaCN, supposedly going through 3-methylidene-3*H*-indol-1-ium species [27]. It was observed that LiAlH₄ reduction of halogenated indole-3-carbonitriles resulted in partial dehalogenation of indole. Due to slight differences in the polarity of tryptamine and halotryptamines resulting in poor chromatography separation, a milder method was used instead. Indole-3-carbonitriles were converted into the corresponding primary amines using a mixture of AlCl₃ and LiAlH₄. The reductive amination with NaBH₄ after imine formation allowed us to obtain the final products of *N*-skatyltryptamines in good yields. The spectral data and chromatograms can be found in Supplementary Materials.



Scheme 1. a: 1. NaBH_4 , HCONH_2 , MeOH 2. NaCN ; b: AlCl_3 , LiAlH_4 , Et_2O ; c: POCl_3 , DMF; d: NaBH_4 , MeOH.

2.2. Structure–Affinity Relationship

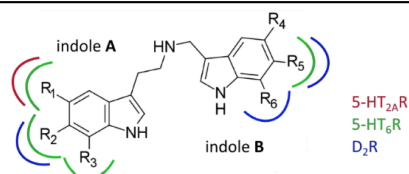
Compound **1**, [2-(1*H*-indol-3-yl)ethyl][(1*H*-indol-3-yl)methyl]amine, exhibited high affinity for 5-HT_{2A} and medium for the 5-HT₆ receptor (K_i 5-HT_{2A} = 20 nM and K_i 5-HT₆ = 172 nM, Table 1—preferred substitution patterns shown in color). Modification of position 5 of the tryptamine motif resulted in a decreased 5-HT_{2A}R affinity (entries 2–4), while 5-HT₆ affinity was slightly increased. 5-Methoxytryptamine derivative **3** was also bound 5-HT_{1A}R with considerable potency (K_i = 156 nM). Compound **5** with the chlorine atom in R2 showed a moderate affinity for 5-HT₆R and D₂R (K_i = 187 nM and 155 nM, respectively). A halogen atom (F, Cl or Br) introduced in position R3 resulted in compounds selective toward the 5-HT₆ receptor (**6**: K_i = 168 nM, **7**: K_i = 133 nM, **8**: K_i = 161 nM). Position R4 substituted with a hydroxyl group or a halogen atom (F, Cl, I) gave compounds with low affinity for 5-HT₆R (entries 9–12). Compound **13** with a fluorine atom in R5 showed low affinity for 5-HT₆R (K_i = 225 nM) and D₂R (K_i = 299 nM). Substitution of R5 with a chlorine or a bromine atom increased the affinity for 5-HT₆R (**14**: K_i = 90 nM, **15**: K_i = 102 nM); in addition, compound **14** was also bound to D₂R (K_i = 124 nM). Introducing the halogen atom in position R6 resulted in compounds that exhibited a high affinity only for the D₂ receptor (**16**: K_i = 91 nM, **17**: K_i = 51 nM, **18**: K_i = 55 nM). Benzyloxy substitution in R6 (**19**) gave compounds with weak affinity for 5-HT₆R (K_i = 303 nM). Disubstituted compounds were synthesized combining a 5-methoxytryptamine fragment with broad serotonin receptor affinity with an aldehyde component bearing a halogen atom that was thought to trigger D₂R antagonism, while not interfering with 5-HT₆R binding. The resulting compounds were thus substituted at both indole fragments with a methoxy at R1 and a chlorine at either R5 or R6 and exhibited high binding affinity for 5-HT₆R (K_i = 98 nM and K_i = 53 nM, respectively) as for 5-HT_{1A}R (K_i = 79 nM and K_i = 187 nM, respectively), but did not bind to D₂R.

2.3. Functional Assays toward 5-HT₆R and D₂R

For the compounds with the highest binding affinity for 5-HT₆R and D₂R, intrinsic function toward 5-HT₆R in agonistic and antagonistic mode and for D₂R in antagonistic mode were evaluated (Table 2). Substitution in position R6 acted as an agonism switch for 5-HT₆R, with compound **18** exhibiting EC_{50} 5-HT₆ = 77 nM. Switching from bromine to chlorine, and substitution with a methoxy group in position 5 of the tryptamine motif in compound **22** resulted in enhanced potency (EC_{50} 5-HT₆ = 26 nM), while the substitution pattern was R1 = methoxy, and R6 = chlorine comparable potency (**21**, EC_{50} 5-HT₆ = 22 nM).

For the D₂ receptor, only the antagonistic function was observed for all the tested entries. The most efficacious were *N*-skatyltryptamines with halogens in positions R2 (**5**, EC_{50} = 104 nM) and R5 (**13** and **15**, EC_{50} = 91 nM and EC_{50} = 109 nM), respectively.

Table 1. Binding affinities K_i of the synthesized compounds. Substitutions, which resulted in an increased affinity were marked in the Markush structure with arcs: 5-HT_{2A}R—red, 5-HT₆R—green, D₂R—blue.



ID	R1	R2	R3	R4	R5	R6	pK _i [nM]				
							5-HT _{1A}	5-HT _{2A}	5-HT ₆	5-HT ₇	D ₂
Trp	H	H	H	-	-	-	7.16	6.51	6.95	7.22	<5.00
5-MeOTrp	MeO	H	H	-	-	-	9.05	7.35	7.92	6.32	6.18
5-Cl-Trp	Cl	H	H	-	-	-	8.80	7.50	8.42	8.80	6.61
1	H	H	H	H	H	H	6.82	8.70	7.76	5.54	7.22
2	Me	H	H	H	H	H	7.16	7.25	7.89	6.53	<5.00
3	OMe	H	H	H	H	H	7.81	8.08	7.93	7.25	6.49
4	Cl	H	H	H	H	H	n.d.	n.d.	7.97	n.d.	6.61
5	H	Cl	H	H	H	H	6.48	6.93	7.78	5.80	7.81
6	H	H	F	H	H	H	6.56	7.42	7.77	5.99	6.53
7	H	H	Cl	H	H	H	6.29	7.20	7.88	5.60	5.93
8	H	H	Br	H	H	H	6.22	7.11	7.79	5.69	6.52
9	H	H	H	OH	H	H	6.54	6.71	6.65	6.29	6.12
10	H	H	H	F	H	H	7.31	6.46	7.39	6.32	6.07
11	H	H	H	Cl	H	H	7.17	6.49	7.29	6.42	6.68
12	H	H	H	I	H	H	7.31	6.63	7.34	6.29	6.68
13	H	H	H	H	F	H	6.87	6.59	7.65	5.74	7.52
14	H	H	H	H	Cl	H	6.97	7.33	8.05	5.80	7.91
15	H	H	H	H	Br	H	7.01	6.39	7.99	6.33	7.54
16	H	H	H	H	H	F	6.25	6.91	7.50	5.89	8.04
17	H	H	H	H	H	Cl	7.55	6.41	7.44	6.97	8.29
18	H	H	H	H	H	Br	7.52	6.40	7.35	6.88	8.26
19	H	H	H	H	H	OBn	7.13	6.64	7.52	5.95	6.39
20	OMe	H	H	H	H	Cl	8.10	7.51	8.01	7.53	6.63
21	OMe	H	H	H	Cl	H	7.73	7.76	8.28	7.09	6.81
22	H	Cl	H	H	H	Cl	6.25	6.39	7.44	5.88	6.30

n.d.—not determined.

Table 2. Determined EC₅₀ and K_b values for the selected compounds.

ID	R ₁	R ₂	R ₃	R ₄	R ₅	R ₆	5-HT ₆ EC ₅₀	5-HT ₆ K _b	D ₂ K _b
							[nM]		
1	H	H	H	H	H	H	n.d.	151	n.d.
5	H	Cl	H	H	H	H	157	136	104
13	H	H	H	H	F	H	n.d.	30	91
14	H	H	H	H	Cl	H	n.d.	112	290
15	H	H	H	H	Br	H	n.d.	131	109
17	H	H	H	H	H	Cl	n.d.	234	215
18	H	H	H	H	H	Br	77	10,000	167
21	OMe	H	H	H	H	Cl	22	10,000	n.d.
22	OMe	H	H	H	Cl	H	26	n.d.	n.d.

n.d.—not determined.

2.4. Molecular Modeling

Functional assays showed that small structural changes caused significant differences in intrinsic function, thus the binding mode of compounds **15** and **18** was investigated to find the plausible molecular recognition site. Structures of compounds were docked to 5-HT₆R homology models built on the β₂ adrenergic receptor crystal structure as a template and to

the D₂ receptor (PDB ID: 6CM4). The QPLD was used to obtain ligand–receptor complexes, since this algorithm describes the anisotropy of the electron density of halogen atoms. In the acquired complexes, the bromine substituent played different roles in binding to the D₂ and 5-HT₆ receptors. Analysis of the binding modes showed that in the D₂ binding site (Figure 1A), the bromine can be involved in the weak halogen bonds with D3.32 and Y7.43 side chains only for the 6-Br derivative. Both derivatives showed a similar binding mode to the pose of the risperidone from the crystal structure of the D₂R complex (Figure 1A). However, the bromine in the 5-HT₆R (Figure 1B) did not show any specific interactions, and it seems that in both derivatives, bromine plays a steric function (fitting to the shape of the binding site). These observations are in line with the in vitro data.

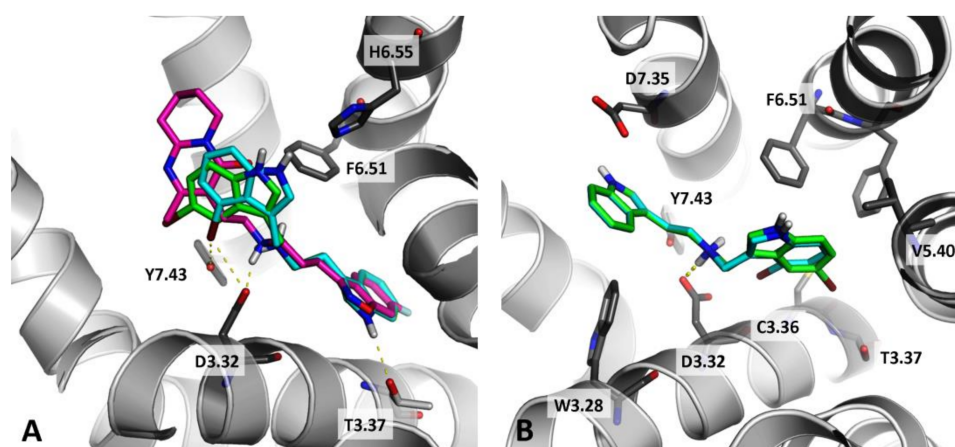


Figure 1. Illustration of the binding modes of selected compounds in the binding site of D₂ and 5-HT₆Rs. Comparison of binding modes of compound **15** (green), **18** (cyan) vs. risperidone (magenta) in D₂R (A), and **15** vs. **18** in 5-HT₆R (B).

The structure–5-HT₆R function relationship could not be analyzed based on the acquired complexes. The agonist–antagonist switch observed for the **15** and **18** pair could have been caused by the stabilization of the “flipped” ligand pose (i.e., with the skatyl fragment pointing down to the intracellular part of the receptor), presumably resulting in receptor antagonism. This, however, is a hypothesis that would need extensive, additional studies to confirm.

2.5. In Vitro ADMETox Studies

2.5.1. Permeability Assay

The most common screening method to define compound permeability is the parallel artificial membrane permeability assay (PAMPA). This test allows one to determine the compounds’ passive penetration through the bilayer artificial membranes that mimic the barrier between the intestine wall and blood. Caffeine was used as a reference compound with high *Pe* value ($Pe = 15.1 \times 10^{-6}$ cm/s) and norfloxacin as a compound with very poor *Pe* value ($Pe = 0.56 \times 10^{-6}$ cm/s). All tested chlorine derivatives (**5**, **14**, and **17**) exhibited medium permeability coefficients (*Pe*) compared to caffeine (Table 3). However, compounds with the bromine substituent, **15** and **18**, showed rather low *Pe* value but still higher than norfloxacin ($Pe = 2.42 \times 10^{-6}$ cm/s and $Pe = 3.90 \times 10^{-6}$ cm/s for **15** and **18**, respectively).

2.5.2. Metabolic Stability

To determine the most probable metabolite structures, compounds **5**, **14**, **15**, **17**, and **18** were incubated with MLMs (mouse liver microsomes) for prolonged time and mass spectra of the obtained mixtures were recorded. In the next step, MetaSite 6.01 software was applied to visualize the obtained in vitro data. In silico predictions indicated that the most probable biotransformation for *N*-skatyltryptamines is hydroxylation, which was in agreement with the in vitro experiment. The molecular masses and predicted products of metabolism

are shown in Table 4. Almost all compounds were converted into two hydroxylated metabolites, except of compound 5, which showed only one hydroxylated metabolite.

Table 3. Permeability coefficients for the tested compounds.

Compound	PAMPA Pe * [10^{-6} cm/s] \pm SD
Norfloxacin	0.56 \pm 0.13
Caffeine	15.1 \pm 0.40
5	7.09 \pm 1.24
14	8.34 \pm 1.33
15	2.42 \pm 0.92
17	8.42 \pm 0.27
18	3.90 \pm 0.56

* tested in triplicate.

Table 4. Molecular masses of the tested compound and retention times and molecular mass of the metabolite and the most probable metabolic pathways of the hit compounds.

Compound	Molecular Mass (m/z)	Retention Time (min)	Molecular Mass of the Metabolite (m/z)	Metabolic Pathway
5	324.25	4.17	M1 340.26	hydroxylation
14	324.31	4.054.38	M1 340.26 M2 340.33	hydroxylation hydroxylation
15	370.13	4.124.34	M1 386.15 M2 384.09	hydroxylation hydroxylation
17	324.25	3.954.27	M1 340.26 M2 340.26	hydroxylation hydroxylation
18	368.14	4.004.27	M1 384.09 M2 386.08	hydroxylation hydroxylation

The hydroxylation of 5 was predicted to occur in position R5 (the aldehyde component derived indole fragment). For compounds with the unsubstituted tryptamine part of the molecule, the addition of hydroxyl group is indicated in the R2 position (Figures 2 and 3). The remaining structures of predicted metabolites can be found in Supplementary Materials.

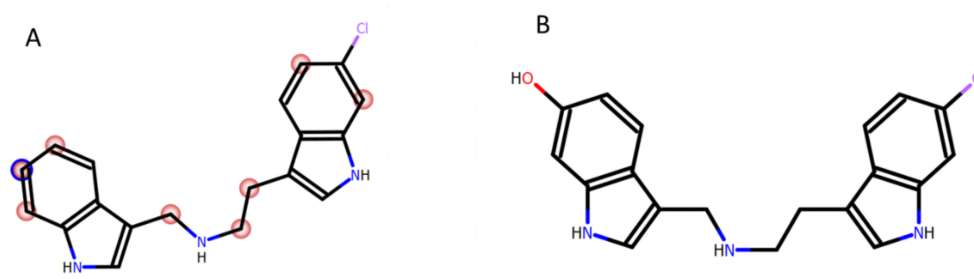


Figure 2. (A) Prediction of the sites of metabolism by MetaSite 6.01. Blue circle marked on the functional group structures indicates the highest biotransformation probability. The fading red color shows decreased probability of metabolism. (B) The most probable structure of 5 main metabolite.

2.5.3. CYP450 Inhibition

CYP2D6 inhibition is quite common for CNS drugs including antipsychotics such as sertindole [28]. The influence of compounds 5, 14, 15, 17, and 18 on CYP450 isoforms CYP3A4 and CYP2D6 were evaluated (Figure 4). In comparison to ketoconazole, which was used as the reference inhibitor of CYP3A4, compounds 14, 15, 17, and 18 only slightly inhibited the activity of this isoform. In contrast, 5 acted as an inducer of CYP3A4. Regarding CYP2D6, all the tested compounds completely inhibited the activity of this isoform, which may result in potential drug–drug interactions.

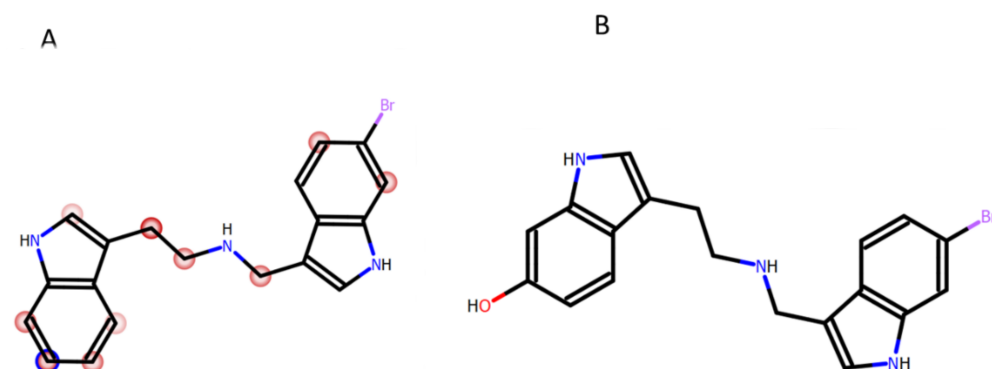


Figure 3. (A) Prediction of the sites of metabolism by MetaSite 6.01. Blue circle marked on the functional group structures indicates the highest biotransformation probability. The fading red color shows decreased metabolism probability. (B) The most probable structure of 15 main metabolite.

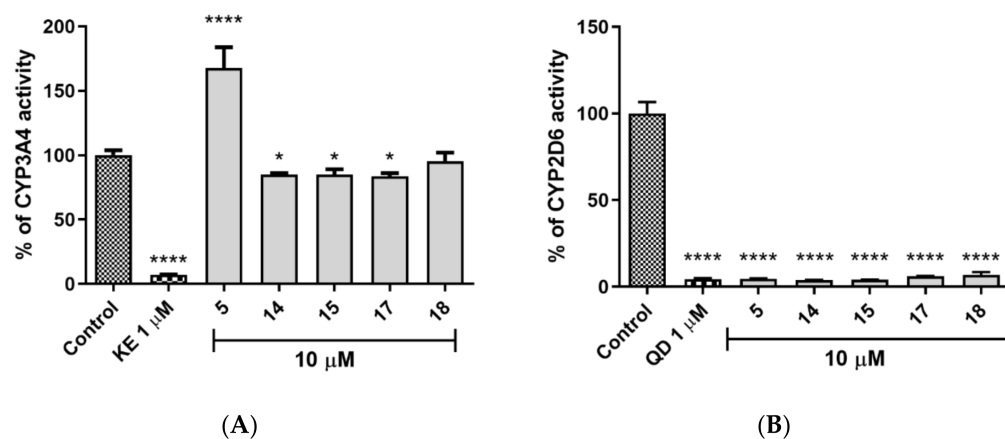


Figure 4. (A) Effect of reference inhibitor ketoconazole and 5, 14, 15, 17, 18 on CYP3A4 activity. Statistical significance (**** $p < 0.0001$, * $p < 0.05$) was analyzed by Graph Pad Prism 8.0.1 software using one-way ANOVA and Bonferroni's multiple comparison post-test. The compounds were examined in triplicate. (B) Effect of reference inhibitor quinidine and 5, 14, 15, 17, and 18 on CYP2D6 activity. Statistical significance (**** $p < 0.0001$) was analyzed by Graph Pad Prism 8.0.1 software using one-way ANOVA and Bonferroni's multiple comparison post-test. The compounds were examined in triplicate.

2.5.4. Hepatotoxicity

To investigate the hepatotoxicity of the new 5-HT₆/D₂ ligands, a cell-based assay using the HepG2 line was conducted. Compounds 5, 14, and 17 at 1 μ M concentration showed a slight antiproliferative effect, where the cell viabilities were decreased to up to ~80% of the control (Figure 5). For bromo-derivatives 15 and 18 at 1 μ M concentration, a proliferative effect was observed, but it was not statistically significant. All the higher concentrations of all compounds (10 μ M, 50 μ M, 100 μ M) caused total cell death, clearly pointing to hepatotoxicity.

2.6. In Vivo Behavioral Tests

2.6.1. MK-801-Induced Hyperactivity in Mice

Agitation, which is characteristic for schizophrenia-like behavior, can be modeled by the administration of NMDA antagonist MK-801. The potential antipsychotic activity of compounds 15 and 18 was thus evaluated in a MK-801-induced hyperactivity model in mice. The administration of MK-801 (0.35 mg/kg) significantly increased the activity of the mice compared to the control group ($p < 0.05$) in all doses. None of the tested compounds reversed MK-801-elevated activity (Figure 6).

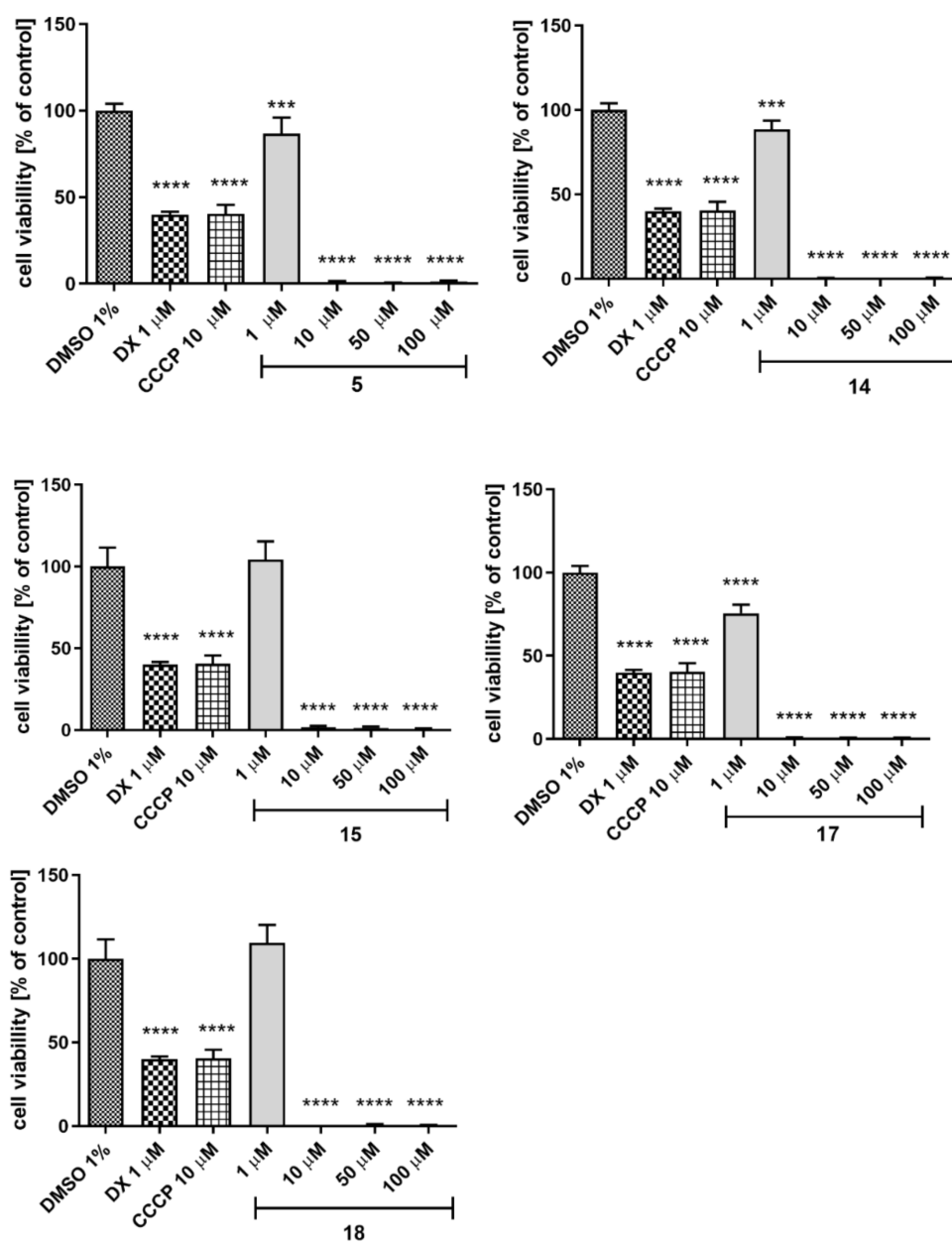


Figure 5. The effect of tested compounds (5, 14, 15, 17, and 18) on the viability of the HepG2 cell line. DMSO 1% in cell growth media (vehicle) was used as the control. Reference cytostatic drug doxorubicin (DX, 1 μM) and mitochondrial toxin CCCP were used as positive controls. Statistical significance (**** $p < 0.0001$, *** $p < 0.001$) was analyzed by Graph Pad Prism 8.0.1 software using one-way ANOVA and Bonferroni's multiple comparison post-test. The compounds were examined in quadruplicate.

2.6.2. Novel Object Recognition (NOR) Test

The effect of acute treatment with compounds 15 and 18 on the cognitive function in the novel object recognition test in mice was checked (Figure 7). Compound 15 reversed memory impairment induced by MK-801 (0.3 mg/kg) at doses of 0.5 and 1 mg/kg ($p < 0.01$, $p < 0.0001$), but not at 3 mg/kg. Compound 18 reversed memory impairment induced by MK-801 (0.3 mg/kg) at all tested doses (0.1; 0.5; 1 mg/kg); $p < 0.0001$, $p < 0.0001$, $p < 0.01$.

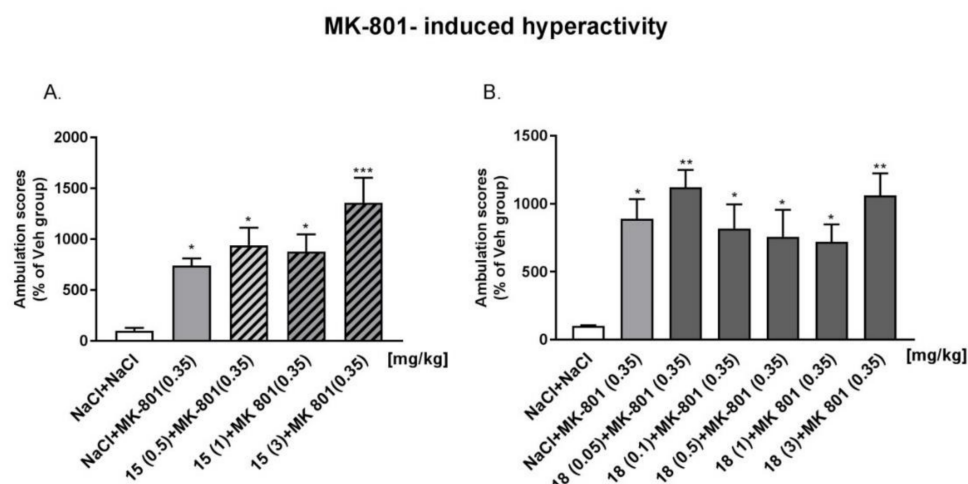


Figure 6. (A) Effect of compound **15** (0.5, 1, 3 mg/kg) and (B) **18** (0.05, 0.1, 0.5, 1, 3 mg/kg) on MK-801-induced hyperactivity in Albino Swiss mice. The test compounds were given 30 min before MK-801 administration, which was given 30 min before the test. Locomotor activity was monitored over a 60 min session immediately following an injection of MK-801. The data are presented as mean \pm SEM, $n = 5$ –8 mice per group. Data were analyzed with one-way ANOVA and Newman–Keuls post-hoc. **15**: $F(4, 29) = 5.293$, $p = 0.0025$; **18**: $F(6, 43) = 3.653$, $p = 0.005$; * $p < 0.05$; ** $p < 0.01$; *** $p < 0.001$ vs. NaCl + NaCl (Veh group).

Novel object recognition test

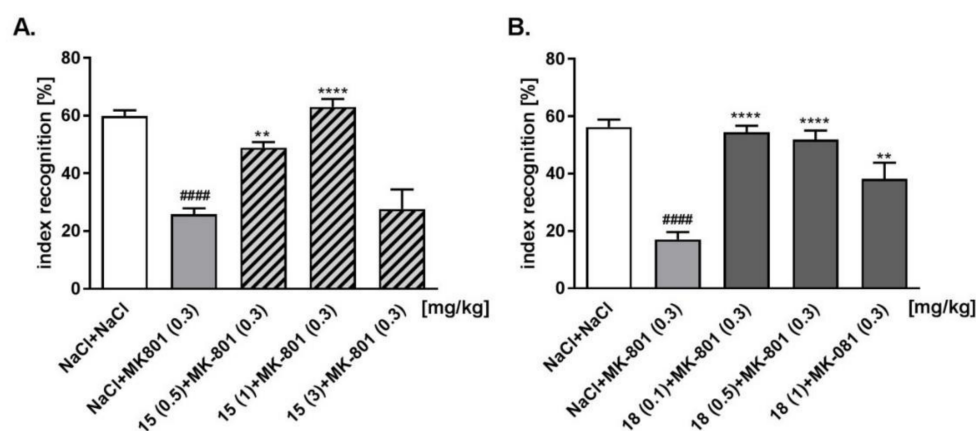


Figure 7. Novel object recognition test in mice. Effectivity of **15** (A) and **18** (B). Bars represent the means \pm SEM, $n = 5$ –10. Data were analyzed with one-way ANOVA and Newman–Keuls post-hoc. **15**: $F(4, 33) = 18.88$, $p < 0.0001$; **18**: $F(4, 35) = 12.45$, $p < 0.0001$; #### $p < 0.0001$ vs. Con; ** $p < 0.01$, **** $p < 0.0001$.

2.6.3. Effect of Compound **15** and **18** on Spontaneous Activity of Mice

Compound **15** administered at the doses of 0.5, 1, and 3 mg/kg did not affect the locomotor activity of mice (Table 5, $p > 0.05$). Similarly, compound **18** administered at the doses of 0.05, 0.1, 0.5, 1, and 3 mg/kg did not influence the spontaneous locomotor activity of mice ($p < 0.05$).

Mice were placed separately into activity cages for an acclimatization period of 30 min, then they were injected i.p. with compound **15** (0.5, 1, and 3 mg/kg) or compound **18** (0.05, 0.1, 0.5, 1, and 3 mg/kg, respectively). After a further 30 min, they were injected with saline (10 mL/kg). From this point on, the ambulation scores were measured for 60 min. The data are presented as mean \pm SEM, $n = 5$ mice per group. Data were analyzed with one-way ANOVA and Dunnett's post-hoc. **15**: $F(3, 16) = 1.225$, $p = 0.333$; **18**: $F(5, 24) = 0.791$, $p = 0.567$.

Table 5. Effect of compound **15** and **18** on the spontaneous activity of mice.

Compounds	Doses (mg/kg)	Ambulation Scores \pm SEM
NaCl	-	100.0 \pm 11.81
15	0.5	134.9 \pm 11.13
15	1	124.7 \pm 21.75
15	3	91.8 \pm 24.61
NaCl	-	100.0 \pm 8.95
18	0.05	113.6 \pm 34.00
18	0.1	131.8 \pm 19.50
18	0.5	116.7 \pm 13.23
18	1	85.31 \pm 15.86
18	3	87.79 \pm 20.89

3. Discussion

There have been reports of potent 5-HT receptor ligands belonging to the class of *N*-arylmethyl arylethylamines dating back to 1994 [29]. The exploration of this chemical was fueled by the discovery of ultrapotent 5-HT_{2A}R agonists with hallucinogenic activity: *N*-benzyl[2-(2,5-dimethoxyphenyl) ethyl]amines. Despite relatively very high selectivity, the so called NBOMe compounds also bound to 5-HT_{2B}, 5-HT_{2C}, 5HT₆, and opioid and histamine receptors [30]. The next important entry was the work of Nichols et al. on *N*-benzyl-5-methoxytryptamines, which exhibited high affinity for 5-HT_{2A}R as well as for 5-HT_{2B} and a selectivity over 5-HT_{1A}, 5-HT_{1B}, 5-HT_{1D}, 5-HT_{1E}, 5-HT₃, 5-HT_{5A}, and 5-HT₇ receptors. Three entries: **5b**, **5i**, and **5l** showed remarkable affinity for 5-HT₆R (25, 27, and 10 nM, respectively).

In the presented work, a series of *N*-skatyltryptamines were synthesized and their affinities for 5-HT_{1A}, 5-HT_{2A}, 5-HT₆, 5-HT₇, and D₂ receptors were determined. The study commenced with the synthesis of **1**, which turned out to be a 5-HT_{2A}R partial agonist. Halogen substitution was applied to the parent compound **1** in order to search for positions enabling contacts with halogen bond acceptors within the receptors. Thus, selective D₂R antagonists were discovered, along with mixed 5-HT_{1A}R, 5-HT₆R, and D₂R antagonists and dual D₂R, 5-HT₆R ligands. 5-HT_{2A}R affinity was observed only in the derivatives of 5-methoxytryptamine. The substitution with a halogen atom in position 6 or 7 (R5 and R6, respectively) of the indole within the skatyl fragment dramatically enhanced D₂R affinity, while switching between the agonistic (with halogen at R6) and antagonistic (with halogen at R5) function at 5-HT₆R. Disubstituted derivatives **21** and **22** acted as potent and selective 5-HT₆R agonists. The ADMET study showed that despite expectations, free tryptamine fragments were not detected after prolonged incubation with mouse liver microsomes, with hydroxylation being the most prevalent metabolic pathway. The PAMPA model revealed a rather high passive permeability of the studied compounds. Although useful as molecular probes, *N*-skatyltryptamines turned out to be hepatotoxic, thus not suitable to further development as pharmaceutical drugs. The tested compounds were also strong inhibitors of CYP2D6 isoforms, indicating possible drug–drug interactions. The pharmacological profile of compounds **15** and **18** resembled that of atypical antipsychotics (Figure 8).

This pair of isomers differed by 5-HT₆R function with **15** being an antagonist and **18** an agonist. It was thus a good opportunity to settle how a combination of D₂R antagonist and 5-HT₆R agonist or antagonist differed in behavioral models of psychosis and cognitive impairment. Contrary to antipsychotic drugs clozapine or haloperidol [32], **15** and **18** did not reverse the locomotor activity elevated by the administration of MK-801. The exacerbation of hyperactivity at 3 mg/kg of **15** was not statistically significant. In the novel object recognition test, compound **15** significantly reversed memory impairment after MK-801 administration at 0.5 and 1 mg/kg, while **18** at all doses. Both compounds did not affect spontaneous activity of mice (i.e., did not induce sedation). It is likely that at the tested doses, the 5-HT₆R mediated effect was more apparent than the D₂R blockade. However, at

the 0.3–3 mg/kg range, in the behavioral models used, we could not spot the difference between the 5-HT₆R agonist and antagonist, with both producing a procognitive effect.

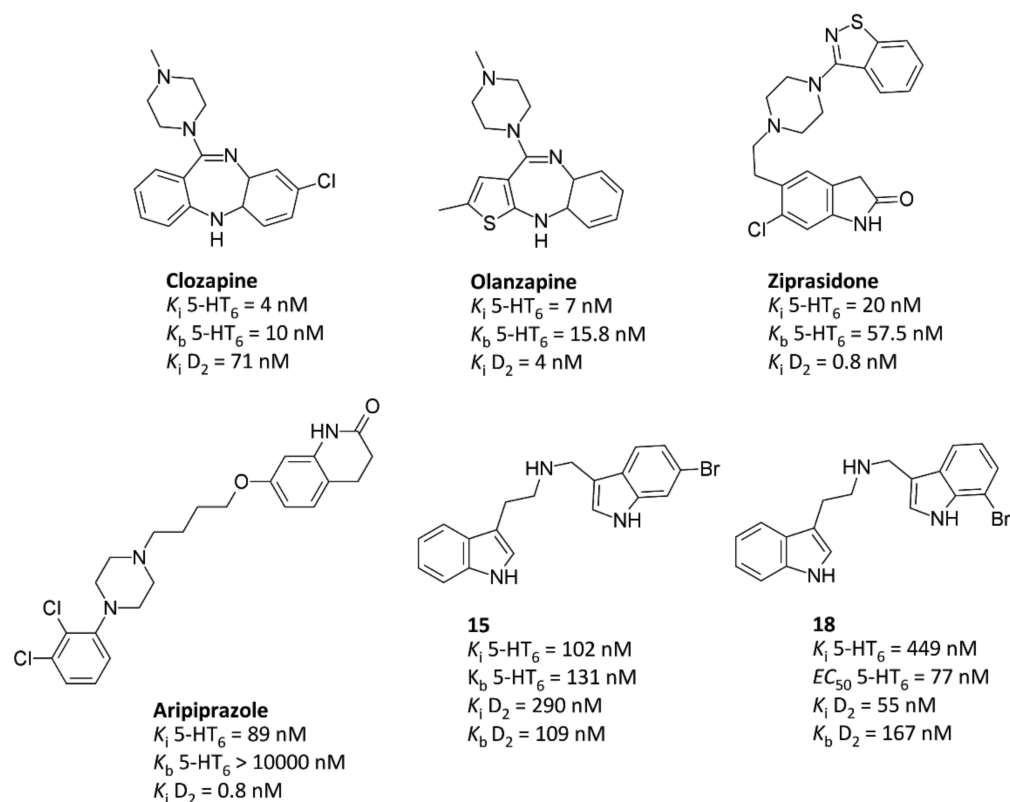


Figure 8. Atypical antipsychotics and the structures of compounds **15** and **18** from this work. Binding affinities of antipsychotic drugs and their antagonist function were taken from the work of Dupuis et al. (2008) [31].

The observed lack of difference in the action of **15** and **18** in the MK-801 impaired NORT may look bizarre. However, there have been reports of paradoxical actions of glutamatergic drugs such as different outcomes in healthy individuals and patients [33,34]. The observed similar effects of compounds **15** and **18** in NORT could possibly be related to the restored BDNF levels described by Rychtyk et al. [20]. The authors showed that both WAY-181187, which is a selective 5-HT₆R agonist and SB-742457, a selective antagonist, alleviated the MK-801-induced inhibition of hippocampal BDNF signaling. There are, however, many other possible explanations since the mechanism of 5-HT₆R ligand cognition enhancement remains elusive. Another proposed hypothesis postulates that agonists activate 5-HT₆ receptors located directly on cholinergic and/or glutamatergic neurons, while antagonists act probably on 5-HT₆ receptors located on GABAergic interneurons [35].

4. Materials and Methods

4.1. Chemistry

Materials. All organic reagents were purchased from Merck and Combi-Blocks and were used without purification. Solvents and inorganic reagents were acquired from Chempur. The reaction progress was monitored by TLC on Merck Silica Gel 60 F 254 on aluminum plates. Column chromatography was performed on Merck Silica Gel 60 (0.063–0.200 mm; 70–230 mesh ASTM).

Analytical methods. UPLC/MS analysis was performed on a Waters TQD spectrometer combined with UPLC Acquity H-Class with a PDA eLambda detector. A Waters Acquity UPLC BEH C18 1.7 μ m 2.1 \times 50 mm chromatographic column was used at 40 $^{\circ}$ C, 0.3 mL/min flow rate, and 1.0 μ L injection volume (the samples were dissolved in LCMS

grade acetonitrile, typically at a concentration of 0.1–1 mg/mL prior to injection). All mass spectra were recorded under electrospray ionization in positive mode (ESI+) and chromatograms were recorded with UV detection in the range of 190–300 nm. The gradient conditions used were: 80% phase A (water +0.1% formic acid) and 20% phase B (acetonitrile +0.1% formic acid) to 100% phase B (acetonitrile +0.1% formic acid) at 3.0 min, kept for 3.5 min, then to initial conditions until 4.0 min, and kept for an additional 2.0 min. Total time of analysis was 6.0 min.

Purity analysis. ^1H and ^{13}C NMR spectra were recorded on a Bruker Avance III HD 500 NMR spectrometer. All samples were dissolved in DMSO- d_6 with TMS as the internal standard. The spectral data of the compounds refer to their free bases or salts.

All presented compounds were of at least 95% purity as determined by LCMS. Syntheses and characterization details for intermediate products and final compounds as well as the spectral data for all compounds are included in the Supplementary Materials.

Software. Marvin Sketch was used to draw the chemical structures, substructures, and reactions, Marvin 19.8.0, ChemAxon. Instant JChem was used for structure searching and chemical database access, Instant JChem 20.20.0, ChemAxon (www.chemaxon.com). Mnova was used to visualize, process, analyze, and report the ^1H and ^{13}C NMR spectra. Mendeley was used for citations (Mendeley Desktop 1.19.4, www.mendeley.com).

General procedure 1 for the synthesis of substituted N-skatyltryptamines (1–23):

To a solution of appropriate tryptamine (2.85 mmol) in 10 mL of methanol there was added a substituted aldehyde (3 mmol) in one portion. The formation of imine was monitored by TLC. After completion of the reaction, NaBH_4 (3.3 mmol) was added in small portions. The mixture was left overnight and then tested by TLC or LCMS. When no imine was observed, 20 mL of water was added and the product was extracted three times with 20 mL of ethyl acetate or chloroform. The organic phases were combined, washed two times with 20 mL of water and once with brine, dried over anhydride magnesium sulfate, and concentrated on a rotavap. The final product was purified via flash chromatography using ethyl acetate:methanol:triethylamine 9:1:0.03 (*v/v/v*).

4.2. In Vitro Pharmacology

4.2.1. Radioligand Binding Assay

Cell Culture. HEK293 cells (ATCC) with the stable expression of human serotonin 5-HT $_{1A}$ R, 5-HT $_6$, and 5-HT $_{7B}$ R or dopamine D $_{2L}$ R (obtained using of Lipofectamine 2000, Invitrogen) or CHO-K1 cells with plasmid containing the sequence coding for the human serotonin 5-HT $_{2A}$ receptor (PerkinElmer) were maintained at 37 °C in a humidified atmosphere with 5% CO $_2$ and were grown in Dulbecco's modified Eagle's medium containing 10% dialyzed fetal bovine serum and 500 $\mu\text{g}/\text{mL}$ G418 sulfate. For the membrane preparations, cells were subcultured into 150 cm 2 cell culture flasks, grown to 90% confluence, washed twice with phosphate buffered saline (PBS) prewarmed to 37 °C, pelleted by centrifugation (200 g) in PBS containing 0.1 mM EDTA and 1 mM dithiothreitol, and stored at –80 °C.

General. To determine affinity of all synthesized compounds for following receptors: 5-HT $_{1A}$ R, 5-HT $_{2A}$ R, 5-HT $_6$, 5-HT $_7$, and D $_2$ radioligand binding assays were conducted. The assays were performed via the displacement of the respective radioligands from the cloned human receptors, all stably expressed in HEK-293 cells (except for 5-HT $_{2A}$ R, which was expressed in CHO cells). The experiments were conducted using 1.5 nM [^3H]-8-OH-DPAT (135.2 Ci/mmol) for 5-HT $_{1A}$ R, 2 nM [^3H]-ketanserin (53.4 Ci/mmol) for 5-HT $_{2A}$ R, 2 nM [^3H]-LSD (83.6 Ci/mmol) for 5-HT $_6$ R, 0.6 nM [^3H]-5-CT (39.2 Ci/mmol) for 5-HT $_7$ R, and [^3H]-raclopride (74.4 Ci/mmol) for D $_2$ R (PerkinElmer, USA). Non-specific binding was defined using 10 mM of 5-HT in the 5-HT $_{1A}$ R and 5-HT $_7$ R binding experiments, whereas 20 mM of mianserin, 10 mM of methiothepine, or 1 mM of (+)-butaclamol was used in the 5-HT $_{2A}$ R, 5-HT $_6$ R, and D $_{2L}$ R assays, respectively. Each compound was tested in triplicate at 7–8 concentrations (10^{-11} – 10^{-4} M). The inhibition constants (K_i) were calculated using

the Cheng–Prusoff equation [36] and the results were expressed as the means of at least two independent experiments.

4.2.2. D₂R Functional Assay

HEK293 cell line with stable expression of human D₂ (prepared with the use of Lipofectamine 2000) was maintained at 37 °C in a humidified atmosphere with 5% CO₂ and was grown in Dulbecco's modified Eagle medium containing 10% dialyzed fetal bovine serum and 500 µg/mL G418 sulfate. For functional experiments, cells were subcultured in 25 cm² flasks, grown to 90% confluence, washed twice with prewarmed to 37 °C phosphate buffered saline (PBS), and centrifuged for 5 min (160 × g). The supernatant was aspirated, and the cell pellet was resuspended in stimulation buffer (1 × HBSS, 5 mM HEPES, 0.5 mM IBMX, 0.1% BSA).

The functional properties of compounds were evaluated using the LANCE Ultra cAMP Detection Kit (PerkinElmer). D₂ receptors in HEK293 cells are coupled to G_i subtype and decreased cAMP production. Cells were stimulated with 1 µM of forskolin (EC₉₀). Each compound was tested in triplicate at eight concentrations (10⁻¹¹–10⁻⁴ M).

For quantification of cAMP levels, cells (5 µL) were incubated with 5 µL mixture of compounds (tested ligand and forskolin with 100 nM quinpirole for antagonist binding mode) for 30 min at room temperature in 384-well white opaque microtiter plate (PerkinElmer). After incubation, the reaction was stopped and cells were lysed by the addition of 10 µL working solution (5 µL Eu-cAMP and 5 µL ULight-anti-cAMP). The assay plate was incubated for 1 h at room temperature. Time-resolved fluorescence resonance energy transfer (TR-FRET) signal was detected by an Infinite M1000 Pro (Tecan) using instrument settings from the LANCE Ultra cAMP Detection Kit manual.

4.2.3. 5-HT₆R Functional Assays

The properties of compounds to inhibit cAMP production induced by a 5-HT₆R agonist 5-CT (1000 nM) was evaluated. Compounds were tested in triplicate at eight concentrations (10⁻¹¹–10⁻⁴ M). The level of cAMP was measured using frozen recombinant 1321N1 cells expressing the Human Serotonin 5-HT₆R (PerkinElmer). Total cAMP was measured using the LANCE cAMP Detection Kit (PerkinElmer), according to the manufacturer's instructions. For quantification of cAMP levels, 2000 cells/well (5 mL) were incubated with a mixture of compounds (5 mL) for 30 min at room temperature in a 384-well white opaque microtiter plate. After incubation, the reaction was stopped and cells were lysed by the addition of 10 mL of working solution (5 mL Eu-cAMP and 5 mL ULight-anti-cAMP) for 1 h at room temperature. Time-resolved fluorescence resonance energy transfer (TR-FRET) was detected by an Infinite M1000 Pro (Tecan) using instrument settings from the LANCE cAMP Detection Kit manual. K_b values were calculated from the Cheng–Prusoff equation specific for the analysis of functional inhibition curves: $K_b = IC_{50} / (1 + A/EC_{50})$ where A represents the agonist concentration; IC₅₀ is the concentration of antagonist producing a 50% reduction in the response to agonist; and EC₅₀ is the agonist concentration that causes half of the maximal response. The agonistic properties of compounds were determined with an analogous procedure, but without stimulation with 5-CT [10,36].

4.3. Molecular Modeling

Molecular Docking. The 5-HT₆R homology models built on the β₂ receptor template (PDB ID: 4LDE) were used in this study [37]. The structure of D₂R in complex with antagonist risperidone (PDB code 6CM4) was retrieved from the Protein Data Bank.

The three-dimensional structures of the ligands were obtained using LigPrep and the appropriate ionization states at pH = 7.4 ± 1.0 were assigned using Epik. The Protein Preparation Wizard was used to assign the bond orders and appropriate amino acid ionization states and to check for steric clashes. The receptor grid was generated (OPLS3 force field) by centering the grid box with a size of 12 Å on the D3.32 side chain. Docking was performed by the quantum-polarized ligand docking (QPLD) procedure implemented

in the Schrodinger Suite. QPLD involves the QM-derived ligand atomic charges in the protein environment at the B3PW91 level with conjunction with the ccpVTZ basis set for Cl and Br and the cc-pVTZ-pp basis set for I-containing ligands. Only the best ten poses per ligand returned by the procedure were considered.

4.4. *In Vitro* ADMETox Studies

Materials. The following compounds: caffeine, carbonyl cyanide 3-chlorophenylhydrazone, doxorubicin, ketoconazole, norfloxacin and quinidine were used in this study as the references and purchased from Sigma-Aldrich (St. Louis, MO, USA).

4.4.1. PAMPA

The permeability of compounds was determined by the Pre-coated PAMPA Plate System Gentest™ (Corning, Tewksbury, MA, USA) similarly to a previously described methodology [38,39]. Caffeine (well-permeable reference), norfloxacin (low-permeable reference), and tested compounds were dissolved in PBS buffer (pH = 7.4) and added to the donor wells (300 µL/well) in a final concentration of 200 µM. PBS in a portion of 200 µL/well was added to the wells. Experiments were conducted in triplicate. Incubation of the PAMPA Plate System took 5 h at room temperature. After that time, 50 µL was aspirated from each well and diluted with 50 µL of solution of internal standard (IS). UPLCMS analyses allowed us to estimate the compounds' concentration in the acceptor and donor wells. The permeability coefficients were determined according to formulas provided by the manufacturer [40].

4.4.2. Metabolic Stability

The murine liver microsomes (MLMs) were purchased from Sigma-Aldrich (St. Louis, MO, USA). To determine metabolic pathways, the tested compounds (50 µM) were incubated with 100 mM Tris-HCl buffer at 37 °C with MLMs (1 mg/mL) and NADPH Regeneration System for 2 h. Reactions were quenched with cold, pure methanol and mixtures were centrifuged 14,000 g for 15 min. The supernatants were analyzed using LCMS. The additional MS ion fragmentation of the product and the substrate were performed to determine the most probable structure of the metabolite.

In silico prediction of metabolic biotransformations was performed by MetaSite 6.0.1 (Molecular Discovery Ltd., Hertfordshire, UK) [41]. The most probable metabolic sites of the tested compounds were determined by a computational liver model of metabolism.

4.4.3. CYP450 Inhibition

The experiments were provided using commercially available luminescent CYP3A4 P450-Glo™ and CYP2D6 P450-Glo™ tests purchased from Promega (Madison, WI, USA). The enzymatic reactions were conducted in polystyrene, flat-bottom Nunc™ MicroWell™ 96-well microplates (Thermo Scientific, Waltham, MA, USA). The assays were carried out according to the procedures provided by the manufacturer, as described previously [38,41,42]. Compounds were tested in triplicate at the final concentrations in a range from 0.01 to 25 µM for both isoforms of CYP450. The references of CYP3A4 and CYP2D6 inhibitors (ketoconazole and quinidine, respectively) were tested in a range from 0.001 to 10 µM. Tested compounds were incubated in 100 mM Tris-HCl buffer separately with CYP3A4 and CYP2D6 membranes and the NADPH Regeneration System for 30 min at room temperature in triplicate. The bioluminescent signal was measured after the addition of the Luciferin Detection Reagent by using a microplate reader EnSpire PerkinElmer (Waltham, MA, USA). Both reagents (NADPH Regeneration System and Luciferin Detection Reagent) were purchased from Promega (Madison, WI, USA).

4.4.4. Hepatotoxicity Assay

To estimate the hepatotoxicity of compounds, the hepatoma HepG2 (ATCC® HB-8065™) cell line was used according to previously described protocols [39,42]. The

CellTiter 96[®] AQueous Non-Radioactive Cell Proliferation Assay was obtained from Promega (Madison, WI, USA). The compounds were tested in quadruplicate at four concentrations (1–100 μ M) for 72 h.

4.5. Behavioral Tests

Animals. Male CD1 mice (Charles River, Germany) weighing 20–25 g at the time of arrival were used in behavioral experiments. Animals were kept under standard laboratory conditions (12:12 light: dark cycle, 22 ± 2 °C) with free access to food and water. Animal welfare has been regularly controlled by a veterinarian and animal welfare committee. After two weeks of acclimatization and handling, the experiments began. Experimental groups consisted of four to 10 animals, depending on the procedure. Drugs were administered intraperitoneally (i.p.) at a volume of 10 mL/kg. Experimental assessments were performed by an observer who was blinded to the treatment conditions. All procedures were conducted in accordance with the European Communities Council Directive of 22 September 2010 (2010/63/EU) and Polish legislation acts concerning animal experimentation and were approved by the II Local Ethics Committee by the Maj Institute of Pharmacology, Polish Academy of Sciences in Krakow (272/2019).

Drugs. MK-801 was purchased from Tocris Bioscience, Bristol, UK. MK-801 was dissolved in 0.9% NaCl. Compounds **15** and **18** were dissolved in 0.9% NaCl. All compounds were administered intraperitoneally (i.p.) in a volume of 10 mL/kg. Vehicle-treated animals received appropriate solvents. Vehicle was administered to animals in any case when drug administration was omitted (e.g., control or MK-801-treated groups).

4.5.1. Novel Object Recognition Test

This procedure was adapted from Nilsson et al. (2007) [43] and performed as described in a previous paper by Cieslik et al. (2018) [44]. Habituation, training, and test trials were performed in a black plastic rectangular arena (40 × 30 × 35 cm) illuminated with a light intensity of 335 lux. During the habituation trial (two consecutive days), each animal was allowed to explore the arena for 10 min. The next day, during the training trial (T1), mice were placed in the arena and presented with two identical objects (red glass cylinder; 6.5 cm in diameter and 4.5 cm high) for 5 min. After 1 h, animals were placed back into the arena for a 5 min test trial, during which one of the previously presented familiar objects was replaced with a novel object (a transparent glass elongated sphere-like object with an orange cap; 5.5 cm in diameter and 8.5 cm high). Time spent exploring (i.e., sniffing or touching) the familiar (T_{familiar}) and novel (T_{novel}) objects was measured by a trained observer, and the recognition index [%] was calculated for each mouse [$(T_{\text{novel}} - T_{\text{familiar}})/(T_{\text{familiar}} + T_{\text{novel}})] \times 100$. Compounds were administered 30 min before MK-801 (0.3 mg/kg), which was administered 30 min before training trial.

4.5.2. MK-801-Induced Hyperactivity

The locomotor activity was recorded individually for each animal in locomotor activity cages (according to Rorick-Kehn et al., 2007a,b) [45,46], with modifications (Wieronska et al., 2012) [47]. The mice were placed individually into activity cages (13 × 23 × 15 cm; Opto-M3; Columbus Instruments) for an acclimatization period of 30 min; then they were injected i.p. with compound **15** (0.5, 1, 3 mg/kg) or compound **18** (0.05, 0.1, 0.5, 1, 3 mg/kg) and placed again in the same cages. After 30 min, all of the mice were injected i.p. with MK-801 at 0.35 mg/kg and once again placed in the same cage. From then on, the ambulation scores were counted for 60 min. All of the groups were compared with the MK-801 control group. The experiment also included a control group treated with NaCl only.

4.5.3. Locomotor Activity of Mice

The locomotor activity was recorded individually for each animal in the OPTO-M3 locomotor activity cages described above. Each cage was surrounded with an array of photocell beams. Interruptions of photo beams resulted in horizontal activity defined as

ambulation scores. Mice were placed separately into activity cages for an acclimatization period of 30 min, then were injected i.p. with compound **15** (0.5, 1, 3 mg/kg) compound **18** (0.05, 0.1, 0.5, 1, 3 mg/kg). After a further 30 min, they were injected with saline (10 mL/kg). From this point on, the ambulation scores were measured for 60 min.

Data Analysis. The data are presented as the means \pm SEM. Statistical analysis of the data was performed using Prism 8. One-way ANOVA, followed by the Newman–Keuls post-hoc comparison test, was used in the analysis of the dose-dependent studies of compounds **15** and **18**. A *p*-value of < 0.05 was considered as statistically significant.

5. Conclusions

A further optimization of substituents might yield compounds with enhanced binding/function for the discussed receptors and more optimal profile. On the other hand, the therapeutic potential of *N*-skatyltryptamines seems doubtful due to the discovered hepatotoxicity. A *clogP* = 3.80 (ChemAxon) was calculated for the unsubstituted derivative **1**, placing the lipophilicity at the border of the preferred range. The discovered series may serve as a pool of new tool compounds with useful receptor profiles for CNS studies.

Supplementary Materials: The following are available online: Syntheses and characterization details for final products, ^1H and ^{13}C NMR spectra, LC-MS spectra, conditions of radioligand binding assay, predicted metabolites, and retention times of tested compounds and its metabolites.

Author Contributions: A.H., A.S.H., B.D. and A.J.B. designed the research. A.H., A.S.H., J.S., R.B. and K.K. synthesized, purified, and characterized the library of compounds. G.S. and T.L. performed binding and functional assays. B.S. and P.C. performed the *in vivo* experiments. G.L. and J.H. conducted the ADMET experiments. R.K. was responsible for the *in silico* experiments. A.H., A.S.H., B.D. and A.J.B. contributed to the writing, review, and revision of the manuscript. All authors have read and agreed to the published version of the manuscript.

Funding: This study was supported by the National Science Center within grants SONATA 2014/15/D/NZ7/01782, OPUS13 2017/25/B/NZ7/02929 and by statutory funds from the Maj Institute of Pharmacology Polish Academy of Sciences.

Conflicts of Interest: The authors declare that they have no known competing financial interests or personal relationships that could have appeared to influence the work reported in this paper.

Sample Availability: Samples of compounds **1–22** are available from the authors.

References

1. Kohen, R.; Metcalf, M.A.; Khan, N.; Druck, T.; Huebner, K.; Lachowicz, J.E.; Meltzer, H.Y.; Sibley, D.R.; Roth, B.L.; Hamblin, M.W. Cloning, characterization, and chromosomal localization of a human 5-HT₆ serotonin receptor. *J. Neurochem.* **1996**, *66*, 47–56. [[CrossRef](#)]
2. Bryan, L.B.; Craigo, S.C.; Choudhary, M.S.; Uluer, A.; Monsma, F.J.; Shen, Y.; Meltzer, H.Y.; Sibley, D.R. Binding of typical and atypical antipsychotic agents to 5-hydroxytryptamine-6 and 5-hydroxytryptamine-7 receptors. *J. Pharmacol. Exp. Ther.* **1994**, *268*, 1403–1410.
3. Glatt, C.E.; Snowman, A.M.; Sibley, D.R.; Snyder, S.H. Clozapine: Selective labeling of sites resembling 5HT₆ serotonin receptors may reflect psychoactive profile. *Mol. Med.* **1995**, *1*, 398–406. [[CrossRef](#)]
4. Schechter, L.E.; Lin, Q.; Smith, D.L.; Zhang, G.; Shan, Q.; Platt, B.; Brandt, M.R.; Dawson, L.A.; Cole, D.; Bernotas, R. Neuropharmacological profile of novel and selective 5-HT₆ receptor agonists: WAY-181187 and WAY-208466. *Neuropsychopharmacology* **2008**, *33*, 1323–1335. [[CrossRef](#)]
5. Bourson, A.; Borroni, E.; Austin, R.H.; Monsma, F.J.; Sleight, A.J. Determination of the role of the 5-HT₆ receptor in the rat brain: A study using antisense oligonucleotides. *J. Pharmacol. Exp. Ther.* **1995**, *274*, 173–180.
6. Axovant Announces Negative Topline Results of Intepirdine Phase 3 MINDSET Trial in Alzheimer’s Disease. Available online: <http://investors.axovant.com/node/7286/pdf> (accessed on 26 September 2017).
7. Fullerton, T.; Binneman, B.; David, W.; Delnomdedieu, M.; Kupiec, J.; Lockwood, P.; Mancuso, J.; Miceli, J.; Bell, J. A Phase 2 clinical trial of PF-05212377 (SAM-760) in subjects with mild to moderate Alzheimer’s disease with existing neuropsychiatric symptoms on a stable daily dose of donepezil. *Alzheimer’s Res. Ther.* **2018**, *10*, 1–10. [[CrossRef](#)]
8. Atri, A.; Frölich, L.; Ballard, C.; Tariot, P.N.; Molinuevo, J.L.; Boneva, N.; Windfeld, K.; Raket, L.L.; Cummings, J.L. Effect of idalopirdine as adjunct to cholinesterase inhibitors on change in cognition in patients with Alzheimer disease three randomized clinical trials. *J. Am. Med. Assoc.* **2018**, *319*, 130–142. [[CrossRef](#)] [[PubMed](#)]

9. Nirogi, R.; Mudigonda, K.; Bhyrapuneni, G.; Muddana, N.R.; Goyal, V.K.; Pandey, S.K.; Palacharla, R.C. Safety, Tolerability and pharmacokinetics of the serotonin 5-HT₆ receptor antagonist, SUVN-502, in healthy young adults and elderly subjects. *Clin. Drug Investig.* **2018**, *38*, 401–415. [[CrossRef](#)] [[PubMed](#)]
10. Canale, V.; Grychowska, K.; Kurczab, R.; Ryng, M.; Keeri, A.R.; Satała, G.; Olejarz-Maciej, A.; Koczurkiewicz, P.; Drop, M.; Blicharz, K.; et al. A dual-acting 5-HT₆ receptor inverse agonist/MAO-B inhibitor displays glioprotective and pro-cognitive properties. *Eur. J. Med. Chem.* **2020**, *208*, 112765. [[CrossRef](#)] [[PubMed](#)]
11. Grychowska, K.; Chaumont-Dubel, S.; Kurczab, R.; Koczurkiewicz, P.; Deville, C.; Krawczyk, M.; Pietruś, W.; Satała, G.; Buda, S.; Piska, K.; et al. Dual 5-HT₆ and D₃ receptor antagonists in a group of 1H-pyrrolo[3,2- c]quinolines with neuroprotective and procognitive activity. *ACS Chem. Neurosci.* **2019**, *10*, 3183–3196. [[CrossRef](#)]
12. Staroń, J.; Kurczab, R.; Warszycki, D.; Satała, G.; Krawczyk, M.; Bugno, R.; Lenda, T.; Popik, P.; Hogendorf, A.S.; Hogendorf, A.; et al. Virtual screening-driven discovery of dual 5-HT₆/5-HT_{2A} receptor ligands with pro-cognitive properties. *Eur. J. Med. Chem.* **2019**, *185*, 111857. [[CrossRef](#)]
13. Marcinkowska, M.; Bucki, A.; Panek, D.; Siwek, A.; Fajkis, N.; Bednarski, M.; Zygmunt, M.; Godyń, J.; Del Rio Valdivieso, A.; Kotańska, M.; et al. Anti-Alzheimer's multitarget-directed ligands with serotonin 5-HT₆ antagonist, butyrylcholinesterase inhibitory, and antioxidant activity. *Arch. Pharm.* **2019**, *352*, 1–10. [[CrossRef](#)]
14. Hatat, B.; Yahiaoui, S.; Lecoutey, C.; Davis, A.; Freret, T.; Boulouard, M.; Claeyen, S.; Rochais, C.; Dallemagne, P. A novel in vivo anti-amnesic agent, specially designed to express both acetylcholinesterase (AChE) inhibitory, serotonergic subtype 4 receptor (5-HT_{4R}) agonist and serotonergic subtype 6 receptor (5-HT_{6R}) inverse agonist activities, with a potential inter. *Front. Aging Neurosci.* **2019**, *11*, 1–14. [[CrossRef](#)]
15. Toublet, F.X.; Lalut, J.; Hatat, B.; Lecoutey, C.; Davis, A.; Since, M.; Corvaisier, S.; Freret, T.; Sopková-de Oliveira Santos, J.; Claeyen, S.; et al. Pleiotropic prodrugs: Design of a dual butyrylcholinesterase inhibitor and 5-HT₆ receptor antagonist with therapeutic interest in Alzheimer's disease. *Eur. J. Med. Chem.* **2021**, *210*, 113059. [[CrossRef](#)] [[PubMed](#)]
16. Zajdel, P.; Kos, T.; Marciniak, K.; Satała, G.; Canale, V.; Kamiński, K.; Hołuj, M.; Lenda, T.; Koralewski, R.; Bednarski, M. Novel multi-target azinesulfonamides of cyclic amine derivatives as potential antipsychotics with pro-social and pro-cognitive effects. *Eur. J. Med. Chem.* **2018**, *145*, 790–804. [[CrossRef](#)] [[PubMed](#)]
17. Morozova, M.A.; Lepilkina, T.A.; Rupchev, G.E.; Beniashvily, A.G.; Burminskiy, D.S.; Potanin, S.S.; Bondarenko, E.V.; Kazey, V.I.; Lavrovsky, Y.; Ivachtchenko, A.V. Add-on clinical effects of selective antagonist of 5HT₆ receptors AVN-211 (CD-008-0173) in patients with schizophrenia stabilized on antipsychotic treatment: Pilot study. *CNS Spectr.* **2014**, *19*, 316–323. [[CrossRef](#)]
18. Woods, S.; Clarke, N.N.; Layfield, R.; Fone, K.C.F. 5-HT₆ receptor agonists and antagonists enhance learning and memory in a conditioned emotion response paradigm by modulation of cholinergic and glutamatergic mechanisms. *Br. J. Pharmacol.* **2012**, *167*, 436–449. [[CrossRef](#)]
19. Meneses, A. Memory formation and memory alterations: 5-HT₆ and 5-HT₇ receptors, novel alternative. *Rev. Neurosci.* **2014**, *25*, 325–356. [[CrossRef](#)]
20. Rychtyk, J.; Partyka, A.; Gdula-Argasińska, J.; Mysłowska, K.; Wilczyńska, N.; Jastrzębska-Więsek, M.; Wesołowska, A. 5-HT₆ receptor agonist and antagonist improve memory impairments and hippocampal BDNF signaling alterations induced by MK-801. *Brain Res.* **2019**, *1722*, 146375. [[CrossRef](#)] [[PubMed](#)]
21. Goff, D.; Coyle, J. The emerging role of glutamate in the pathophysiology and treatment of schizophrenia. *Am. J. Psychiatry* **1983**, *75*, 1367–1377. [[CrossRef](#)] [[PubMed](#)]
22. Nikiforuk, A. Assessment of cognitive functions in animal models of schizophrenia. *Pharmacol. Rep.* **2018**, *70*, 639–649. [[CrossRef](#)] [[PubMed](#)]
23. Bubeniková-Valešová, V.; Horáček, J.; Vrajová, M.; Höschl, C. Models of schizophrenia in humans and animals based on inhibition of NMDA receptors. *Neurosci. Biobehav. Rev.* **2008**, *32*, 1014–1023. [[CrossRef](#)] [[PubMed](#)]
24. Arnt, J.; Bang-Andersen, B.; Grayson, B.; Bymaster, F.P.; Cohen, M.P.; Delapp, N.W.; Giethlen, B.; Kreilgaard, M.; McKinzie, D.L.; Neill, J.C. Lu AE58054, a 5-HT₆ antagonist, reverses cognitive impairment induced by subchronic phencyclidine in a novel object recognition test in rats. *Int. J. Neuropsychopharmacol.* **2010**, *13*, 1021–1033. [[CrossRef](#)] [[PubMed](#)]
25. Manahan-Vaughan, D.; von Haebler, D.; Winter, C.; Juckel, G.; Heinemann, U. A single application of MK801 causes symptoms of acute psychosis, deficits in spatial memory and impairment of synaptic plasticity in rats. *Hippocampus* **2008**, *18*, 125–134. [[CrossRef](#)]
26. Nichols, D.E.; Sassano, M.F.; Halberstadt, A.L.; Klein, L.M.; Brandt, S.D.; Elliott, S.P.; Fiedler, W.J. N-Benzyl-5-methoxytryptamines as Potent serotonin 5-HT₂ receptor family agonists and comparison with a series of phenethylamine analogues. *ACS Chem. Neurosci.* **2015**, *6*, 1165–1175. [[CrossRef](#)]
27. Yamada, F.; Hashimime, T.; Somei, M. Simple one step syntheses of indole-3-acetonitriles from indole-3-carboxaldehydes. *Heterocycles* **1998**, *47*, 509–516.
28. Prior, T.I.; Chue, P.S.; Tibbo, P.; Baker, G.B. Drug metabolism and atypical antipsychotics. *Eur. Neuropsychopharmacol.* **1999**, *9*, 301–309. [[CrossRef](#)]
29. Glennon, R.A.; Dukat, M.; El-Bermawy, M.; Law, H.; De Los Angeles, J.; Teitler, M.; King, A.; Herrick-Davis, K. Influence of amine substituents on 5-HT_{2A} versus 5-HT_{2C} binding of phenylalkyl- and indolylalkylamines. *J. Med. Chem.* **1994**, *37*, 1929–1935. [[CrossRef](#)] [[PubMed](#)]

30. Nichols, D.E.; Frescas, S.P.; Chemel, B.R.; Rehder, K.S.; Zhong, D.; Lewin, A.H. High specific activity tritium-labeled N-(2-methoxybenzyl)-2,5-dimethoxy-4-iodophenethylamine (INBMeO): A high-affinity 5-HT_{2A} receptor-selective agonist radioligand. *Bioorg. Med. Chem.* **2008**, *16*, 6116–6123. [[CrossRef](#)] [[PubMed](#)]
31. Dupuis, D.S.; la Cour, C.M.; Chaput, C.; Verrièle, L.; Lavielle, G.; Millan, M.J. Actions of novel agonists, antagonists and antipsychotic agents at recombinant rat 5-HT₆ receptors: A comparative study of coupling to G α s. *Eur. J. Pharmacol.* **2008**, *588*, 170–177. [[CrossRef](#)]
32. O'Neill, M.F.; Shaw, G. Comparison of dopamine receptor antagonists on hyperlocomotion induced by cocaine, amphetamine, MK-801 and the dopamine D1 agonist C-APB in mice. *Psychopharmacology* **1999**, *145*, 237–250. [[CrossRef](#)]
33. Torrisi, S.A.; Lavanco, G.; Maurel, O.M.; Gulisano, W.; Laudani, S.; Geraci, F.; Grasso, M.; Barbagallo, C.; Caraci, F.; Bucolo, C.; et al. A novel arousal-based individual screening reveals susceptibility and resilience to PTSD-like phenotypes in mice. *Neurobiol. Stress* **2021**, *14*, 100286. [[CrossRef](#)] [[PubMed](#)]
34. Mkrtchian, A.; Evans, J.W.; Kraus, C.; Yuan, P.; Kadriu, B.; Nugent, A.C.; Roiser, J.P.; Zarate, C.A. Ketamine modulates fronto-striatal circuitry in depressed and healthy individuals. *Mol. Psychiatry* **2020**. [[CrossRef](#)] [[PubMed](#)]
35. Ramirez, M.J. 5-HT₆ receptors and Alzheimer's disease. *Alzheimer's Res. Ther.* **2013**, *5*, 1–8.
36. Yung-Chi, C.; Prusoff, W.H. Relationship between the inhibition constant (KI) and the concentration of inhibitor which causes 50 per cent inhibition (I50) of an enzymatic reaction. *Biochem. Pharmacol.* **1973**, *22*, 3099–3108. [[CrossRef](#)]
37. Łażewska, D.; Kurczab, R.; Więcek, M.; Kamińska, K.; Satała, G.; Jastrzębska-Więsek, M.; Partyka, A.; Bojarski, A.J.; Wesołowska, A.; Kieć-Kononowicz, K. The computer-aided discovery of novel family of the 5-HT₆ serotonin receptor ligands among derivatives of 4-benzyl-1,3,5-triazine. *Eur. J. Med. Chem.* **2017**, *135*, 117–124. [[CrossRef](#)]
38. Latacz, G.; Hogendorf, A.S.; Hogendorf, A.; Lubelska, A.; Wierońska, J.M.; Woźniak, M.; Cieślík, P.; Kieć-Kononowicz, K.; Handzlik, J.; Bojarski, A.J. Search for a 5-CT alternative. In vitro and in vivo evaluation of novel pharmacological tools: 3-(1-alkyl-1H-imidazol-5-yl)-1H-indole-5-carboxamides, low-basicity 5-HT₇ receptor agonists. *MedChemComm* **2018**, *9*, 1882–1890. [[CrossRef](#)]
39. Latacz, G.; Lubelska, A.; Jastrzębska-Więsek, M.; Partyka, A.; Marć, M.A.; Satała, G.; Wilczyńska, D.; Kotańska, M.; Więcek, M.; Kamińska, K. The 1,3,5-triazine derivatives as innovative chemical family of 5-HT₆ serotonin receptor agents with therapeutic perspectives for cognitive impairment. *Int. J. Mol. Sci.* **2019**, *20*, 3420. [[CrossRef](#)]
40. Chen, X.; Murawski, A.; Patel, K.; Crespi, C.L.; Balimane, P.V. A novel design of artificial membrane for improving the PAMPA model. *Pharm. Res.* **2008**, *25*, 1511–1520. [[CrossRef](#)]
41. Latacz, G.; Lubelska, A.; Jastrzębska-Więsek, M.; Partyka, A.; Sobiło, A.; Olejarz, A.; Kucwaj-Brysz, K.; Satała, G.; Bojarski, A.J.; Wesołowska, A. In the search for a lead structure among series of potent and selective hydantoin 5-HT_{7R} agents: The drug-likeness in vitro study. *Chem. Biol. Drug Des.* **2017**, *90*, 1295–1306. [[CrossRef](#)]
42. Latacz, G.; Lubelska, A.; Jastrzębska-Więsek, M.; Partyka, A.; Kucwaj-Brysz, K.; Wesołowska, A.; Kieć-Kononowicz, K.; Handzlik, J. MF-8, a novel promising arylpiperazine-hydantoin based 5-HT₇ receptor antagonist: In vitro drug-likeness studies and in vivo pharmacological evaluation. *Bioorg. Med. Chem. Lett.* **2018**, *28*, 878–883. [[CrossRef](#)] [[PubMed](#)]
43. Nilsson, M.; Hansson, S.; Carlsson, A.; Carlsson, M.L. Differential effects of the N-methyl-d-aspartate receptor antagonist MK-801 on different stages of object recognition memory in mice. *Neuroscience* **2007**, *149*, 123–130. [[CrossRef](#)] [[PubMed](#)]
44. Cieślík, P.; Woźniak, M.; Kaczorowska, K.; Brański, P.; Burnat, G.; Chocyk, A.; Bobula, B.; Gruca, P.; Litwa, E.; Pałucha-Poniewiera, A. Negative allosteric modulators of mGlu7 receptor as putative antipsychotic drugs. *Front. Mol. Neurosci.* **2018**, *11*, 1–14. [[CrossRef](#)]
45. Rorick-Kehn, L.M.; Johnson, B.G.; Knitowski, K.M.; Salhoff, C.R.; Witkin, J.M.; Perry, K.W.; Griffey, K.I.; Tizzano, J.P.; Monn, J.A.; McKinzie, D.L.; et al. In vivo pharmacological characterization of the structurally novel, potent, selective mGlu_{2/3} receptor agonist LY404039 in animal models of psychiatric disorders. *Psychopharmacology* **2007**, *193*, 121–136. [[CrossRef](#)] [[PubMed](#)]
46. Rorick-Kehn, L.M.; Johnson, B.G.; Burkey, J.L.; Wright, R.A.; Calligaro, D.O.; Marek, G.J.; Nisenbaum, E.S.; Catlow, J.T.; Kingston, A.E.; Giera, D.D. Pharmacological and pharmacokinetic properties of a structurally novel, potent, and selective metabotropic glutamate 2/3 receptor agonist: In vitro characterization of agonist (–)-(1R,4S,5S,6S)-4-amino-2-sulfonylbicyclo[3.1.0]-hexane-4,6-dicarboxylic acid. *J. Pharmacol. Exp. Ther.* **2007**, *321*, 308–317. [[CrossRef](#)] [[PubMed](#)]
47. Wierońska, J.M.; Stachowicz, K.; Acher, F.; Lech, T.; Pilc, A. Opposing efficacy of group III mGlu receptor activators, LSP1-2111 and AMN082, in animal models of positive symptoms of schizophrenia. *Psychopharmacology* **2012**, *220*, 481–494. [[CrossRef](#)]